PHYSICAL REVIEW B VOLUME 32, NUMBER 9 1 NOVEMBER 1985

Dissipation in combined normal and superfluid flows of He II: A unified description

Marie L. Baehr and J. T. Tough
Department of Physics, The Ohio State University, Columbus, Ohio 43210
(Received 2 May 1985)

We have measured the dissipation associated with superfluid turbulence in circular tubes for combined normal and superfluid flows spanning the V_n-V_s plane from pure superflow to thermal counterflow. For relatively small values of V_n the dissipation is consistent with a homogeneous distribution of quantized vortex lines in the superfluid if it is assumed the lines are dragged by the normal-fluid flow. For larger values of V_n this unified description is destroyed by the phenomenon associated with the TI-TII transition in thermal counterflow.

I. INTRODUCTION

It is now generally accepted that the large dissipation associated with the flow of liquid He II through small tubes is the result of an interaction between the normal-fluid excitations and a random array of quantized vortex lines in the superfluid.[1] The condition of superfluid turbulence then can be described in terms of the macroscopic dissipation that is present in a flow, or the particular distribution of quantized vortex lines that is present. A major problem in the description of superfluid turbulence has been the observation that apparently different states of turbulence are produced in different physical situations. In pure superflow the dissipation is independent of tube shape[2,3] suggesting the turbulence is homogeneous. In thermal counterflow, where the superfluid flow is accompanied by a flow of the normal component in the opposite direction, the situation is far more complex. The dissipation depends qualitatively on the tube shape. In tubes of square or circular cross section, the turbulence evolves from a low-density state TI to a high density state TII as the counterflow is increased.[4–6]

Schwarz[7] has shown that it is possible to simulate a state of homogeneous superfluid turbulence with a collection of vortex lines obeying simple dynamical rules. Each line moves under its local self-induced velocity and the normal-fluid friction, while line-line crossing events both randomize the distribution and allow the system to relax into a steady state. The simulated homogeneous vortex line density is in excellent agreement with the dissipation measured in pure superflow experiments,[2,3] and the vortex line density measured in state TII in large tubes.[8] It has not yet been possible to simulate the more complex behavior observed in thermal counterflow associated with the state TI and the TI-TII transition.

The experiments reported in this paper are intended to bridge the gap between the pure superflow results and those in thermal counterflow. We measure the dissipation associated with the superfluid turbulence produced in a small diameter glass tube in which a superfluid flow can be supplemented by a counterflow of the normal fluid at selected velocities. In this way we map out the dissipation in the V_n-V_s plane for all velocity combinations between pure superflow and thermal counterflow. Previous measurements of dissipation in the V_n-V_s plane have been reported by workers at Leiden.[9–12] These pioneering experiments established the global features of the dissipation in the plane, and focused on the oscillatory phenomena found in certain regions. To the extent that our data overlap these previous results the agreement is quite good. Our purpose is to examine in great detail that region of the plane which connects pure superflow with thermal counterflow, and to establish a data base suitable for detailed testing of theoretical predictions. The results are also amenable to phenomenological interpretations which can be useful as a guide to a deeper understanding of the dynamic processes involved in superfluid turbulence. The results also give quantitative descriptions of the vortex line density that can be useful in further experimental studies.

II. APPARATUS

The basic requirements for this experiment are a well characterized flow tube, a method for producing and accurately measuring superfluid and normal-fluid velocities, and good temperature regulation and measuring capabilities. The essential features of the apparatus are shown in Fig. 1. The flow tube connected a large reservoir at temperature T_1 with a small chamber containing a heater H_2. This H_2 chamber was connected to a "fountain pump" consisting of a superleak, heater H_1, and long tube ("fountain pipe"). The superleak prohibited heat flow between the H_1 and H_2 chambers, but allowed the superfluid component of the He II to pass freely. With heater H_1 energized, superfluid was pumped from the reservoir, through the flow tube, and expelled into the main helium bath. The superfluid flow rate through the flow tube, the superfluid velocity V_s, was determined unambiguously from the rate at which the level in the reservoir changed with time. A normal-fluid flow was produced in the flow tube by energizing heater H_2. Since the H_2 chamber was thermally isolated by the superleak and the vacuum space, the heat flux through the flow tube gave the average

 ©1985 The American Physical Society

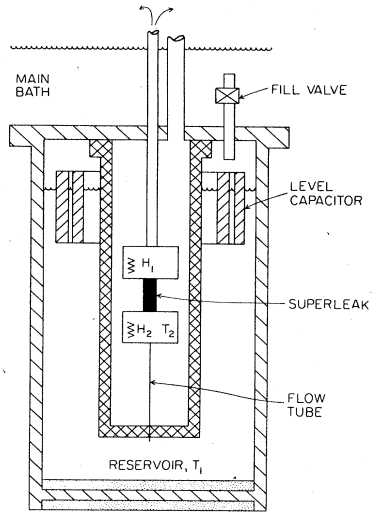

FIG. 1. Details of the apparatus. The H_2 chamber is thermally isolated by a vacuum space and a superleak.

normal-fluid velocity V_n.

The flow tube was identical to the one used in the pure superflow experiments reported previously.[2] A nominally 100 μm i.d. glass tube, 10 cm long was covered with a fiberglass sheath and impregnated with Stycast 1266 epoxy resin. The ends of the encapsulated tube were smoothly dressed and the length was measured to be 9.90 cm. Epoxy reinforced flow tubes have proven to be quite rugged and trouble free. The expansion coefficient of the composite structure was very close to that of the epoxy alone and simplified construction of the apparatus. The vacuum can shown in Fig. 1, as well as the H_1 and H_2 chambers and the fountain pipe, were fabricated from 1266 epoxy. Consequently there was very little thermal stressing of the flow tube when the apparatus was cooled to helium temperatures.

Running the experiment in the thermal counterflow mode only, with the fountain pump heater H_1 off, it was possible to ascertain that the flow tube was functioning properly. If the power dissipated in heater H_2 is $\dot{Q}$, then the two-fluid model gives the average normal-fluid velocity down the tube to be

$$V_n = \dot{Q}/\rho STA \ , \tag{1}$$

where ρ is the HE II density, S the specific entropy, T the average temperature, and A the flow tube area. For sufficiently small values of $\dot{Q}$ the only dissipation is that due to the normal-fluid viscosity η and the temperature difference $\Delta T = T_2 - T_1$ is linear in $\dot{Q}$. The tube diameter d obtained from the slope

$$\frac{\Delta T}{\dot{Q}} = \frac{128\eta l}{\pi d^4 (\rho S)^2 T} \tag{2}$$

is (134 ± 2) μm. This result is quite comparable to the diameters of other tubes from the same lot used previously.[2,4,13] The critical heat currents at the onset of the first turbulent state TI and at the transition to state TII are also in excellent agreement with previous data[4,13] and indicate that the present flow tube is entirely equivalent to those used previously.

A fountain pump was used to produce pure superflow through the flow tube. The term "fountain pump" has traditionally been used to describe any system that produces mass flow using the fountain effect. The essential features of a pump are a long pipe with a constriction on top and a heated chamber on the bottom with a superleak connection to the helium source. With the heater turned on, superfluid is pulled through the superleak by the fountain pressure and is expelled out of the tube by either evaporation or by spilling over the top. In designing the actual fountain pump for our apparatus it was essential to include the effects of "source impedance," that is the influence of the chemical potential of the H_2 chamber on the mass flow rate. We modeled the pump-flow tube system extending the analysis of Broulik and Hess,[14] so that the superfluid velocity through the flow tube V_s was given as a function of the power dissipated by the pump heater H_1 all for a given pipe constriction. The constriction could then be chosen to meet the desired velocity range, the anticipated source chemical potential, and the physical constraints of the apparatus. The majority of the data reported in this paper was obtained with a constriction consisting of 29.5 cm of 0.038-cm i.d. glass tubing. With this constriction we were able to generate superfluid velocities $0 \leq V_s \leq 15$ cm/s over the range of temperature and dissipation encountered in the experiments.

The actual superfluid velocity V_s through the flow tube was determined from the rate of change of the level in the reservoir. A cylindrical level sensing capacitor surrounding the epoxy vacuum can was designed to optimize the velocity determination. The capacitor was 5.7 cm high with a mean gap diameter of 5.3 cm and gap width of 0.042 cm. The ends of the capacitor were electrically guarded, and teflon spacers were employed to assure the gap was uniform. The entire assembly was rigidly supported from the top flange of the reservoir. From the known geometry of the reservoir, capacitor, and flow tube it was possible to calculate the superfluid velocity through the flow tube from the time rate of change of the capacitance $\Delta C/\Delta t$. The capacitor was monitored with a General Radio 1615 capacitance bridge and an Ithaco 393 lock-in amplifier. A small computer was programmed to read the lock-in output for up to about 5 min and display the superfluid velocity. A careful assessment of all the factors involved in the determination of V_s suggests a maximum systematic error of about 5% and a maximum random error of about 0.06 cm/s.

The temperature in the H_2 chamber was determined with a CG500 carbon glass resistor. At 1.6 K this device has a resistance of about 100 KΩ and a sensitivity $\Delta R/R\Delta T$ of about 4.0 K^{-1}. The sensitivity was extremely stable from day to day, and the resistance drift on a given day was of the order of 1 Ω/h. The resistor was monitored with a SHE 120 resistance bridge, adjusted for maximum sensitivity without self-heating. The temperature of the reservoir was electronically regulated using standard techniques. Averaging over 3 s, the fluctuations

were less than 5 μK. We estimate the overall error in determining the temperature difference $T_2 - T_1 = \Delta T$ to be 50 μK.

III. PROCEDURE

The experiments consisted of measurements of the temperature difference ΔT as a function of the velocities V_n and V_s. A simplified diagram of the apparatus is shown in Fig. 2 (upper), and Fig. 2 (lower) shows the region of the V_n-V_s plane accessible to the experiments. Using only the counterflow heater H_2 with the fountain pump off, the trajectory given by the counterflow condition of no net mass flow,

$$\rho_n V_n = -\rho_s V_s \ , \tag{3}$$

is followed in the V_n-V_s plane. Using only the fountain pump with the counterflow heater H_2 off, the pure superflow trajectory ($V_n = 0$) is followed. For appropriate combinations of the fountain pump and the counterflow heater it is therefore possible to study all regions of the V_n-V_s plane between pure superflow and thermal counterflow. In practice we would set the counterflow heater to give a particular value of V_n [Eq. (1)], and keeping this constant, would measure ΔT as the fountain pump was used to change the superfluid velocity V_s. The dashed vertical lines in Fig 2 show the trajectories followed in this procedure.

As mentioned above in Sec. II, we also measured the temperature difference along the thermal counterflow line largely for comparison with previous data to insure the flow tube was well characterized. The present apparatus is not particularly well suited to pure counterflow measurements due to very long time constants encountered when the dissipation is large. Small changes in $\dot{Q}$ produce large changes in ΔT and in the chemical potential of the H_2 chamber. Since the superleak is a chemical-potential short, the level of the helium in the fountain pipe must make a large change, and this is a slow process since the helium must all flow through the superleak. By monitoring the level capacitor however, it was possible to insure that a steady state had been reached before the temperature difference was recorded. When $\dot{Q}$ was sufficiently large, the level of the helium in the fountain pipe was actually pulled below the H_1 chamber, and since no more draining could occur, the time constants for reaching a steady-state temperature difference decreased substantially. Of course when the H_1 chamber is empty, the fountain pump is no longer operational, and this sets an experimental limit on the region of the V_n-V_s accessible in these experiments: We were not able to study the dissipation close to the thermal counterflow line at large values of V_n.

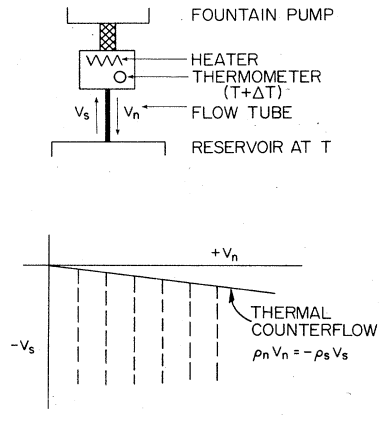

FIG. 2. Schematic diagram of the apparatus showing the directions of the normal-fluid and superfluid flows (upper). Third quadrant of the V_n-V_s plane showing the thermal counterflow trajectory and the experimental trajectories (dashed lines) (lower).

IV. DATA

The temperature difference ΔT was measured as a function of V_n and V_s following the procedure outlined above at bath temperatures of 1.4 and 1.6 K. At 1.4 K we followed the trajectories $V_n = 0$, 2.4, 4.6, 7.4, and 9.7 cm/s. At 1.6 K we followed the trajectories $V_n =$ 0, 0.65, 1.6, 3, 4.9, 5.9, 7, 7.77, 8.28, 8.8, and 9.2 cm/s. We have taken the traditional step of reducing the temperature difference data to give the "equivalent homogeneous vortex line density" L. Essentially L is a measure of the dissipation due to the superfluid turbulence present in the combined V_n-V_s flow. The total temperature difference can be written as the sum of a viscous term and a mutual friction term,

$$\Delta T = \Delta T_\eta + l F_{sn} / \rho_s S \ . \tag{4}$$

The mutual friction force F_{sn} is proportional to the vortex line density L and the relative velocity V between the normal and superfluids,

$$F_{sn} = \tfrac{2}{3}(\rho_n \rho_s / 2\rho)\kappa B V L \ . \tag{5}$$

Here B is the Hall-Vinen coefficient and κ is the quantum of circulation. In the region of the V_n-V_s plane accessible to these experiments (Fig. 2) the two fluids have velocities

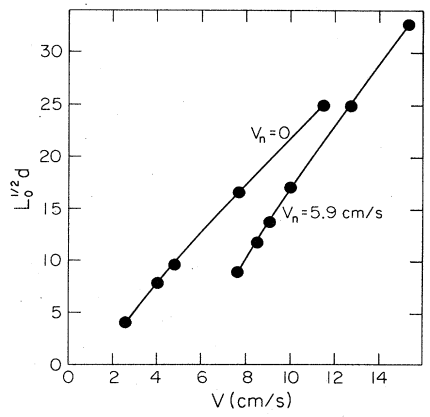

FIG. 3. "Equivalent homogeneous vortex line density" L as a function of the relative velocity V at two different values of the normal fluid velocity at 1.6 K.

of different sign. The magnitude of the relative velocity V is thus the algebraic sum of the magnitudes of the two component velocities

$$V = V_n + V_s \ . \tag{6}$$

Figure 3 gives some representative data, where the temperature difference has been reduced to give the line density L as Eqs. (4) and (5) above. The dimensionless quantity obtained from the product of the square root of the line density times the tube diameter d is actually plotted in this figure. These data were obtained at 1.6 K, for $V_n = 0$ and $V_n = 5.9$ cm/s trajectories in the V_n-V_s plane. The results shown in Fig. 3 are typical of all the different V_n trajectories measured in that the line density (the dissipation) at a given value of the relative velocity V is actually *smaller* at larger V_n. It has been traditional to regard the line density as a function of the relative velocity only. Our data clearly show that this is an oversimplified view of the superfluid turbulence. The line density (or the dissipation) must be considered a function of both V and V_n (or equivalently of V_n and V_s).

It is possible to give all our experimental data in the form shown in Fig. 3, but the result is rather cluttered since there are eleven V_n trajectories at 1.6 K and five at 1.4 K. Furthermore, although this representation of the data most accurately reproduces the actual experimental trajectories, it obscures other cuts through the V_n-V_s plane that may be more revealing. We have chosen instead to give our entire data set in the form of contour plots of $L^{1/2}d$ in the V_n-V_s plane. The results at 1.6 and 1.4 K are given in Figs. 4 and 5, respectively. If the line density only depended on the relative velocity V, the contours of constant $L^{1/2}d$ would be a set of equally spaced, parallel, 45° lines. The extent that the data in Figs. 4 and 5 deviate from this simple picture is an indication of the more complex dependence of the dissipation on the velocities V_n and V_s.

The shaded region near the origin in Figs. 4 and 5 represents an area in the plane where the line density is zero, and there is no measurable mutual friction dissipation. We have discussed this phenomenon and the critical line in the V_n-V_s plane in a previous publication.[15] Another region of interest is found in Fig. 4 (1.6 K) near $V_n = 7$, $V_s = -4$. A rather large distortion of the contour plot occurs in this area, and is associated with the transition from the state TI to TII along the thermal counterflow line. We will postpone discussion of this feature to the end of Sec. V. Generally, however, the contour plots and the dissipation surface they represent are rather featureless, suggesting that the superfluid turbulence varies smoothly in the region between superflow and thermal counterflow.

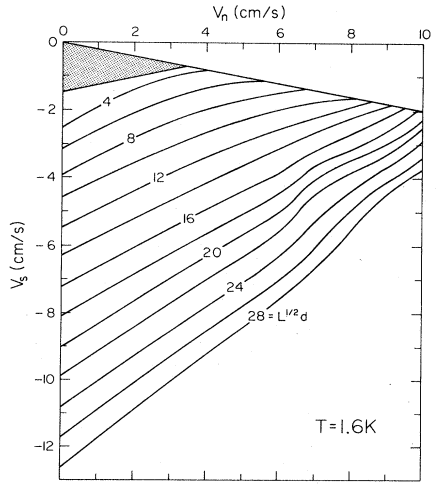

FIG. 4. Contours of constant line density L in the V_n-V_s plane at 1.6 K.

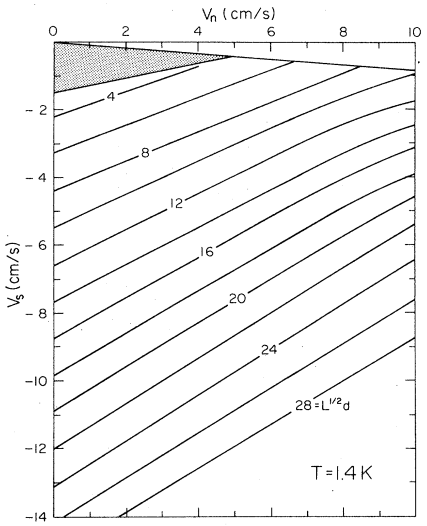

FIG 5. Contours of constant line density L in the V_n-V_s plane at 1.4 K.

V. INTERPRETATION

The experimental results given in Figs. 4 and 5 constitute a solid data base for comparison with future theories or numerical simulations. Lacking these at the present, we have considered various phenomenological interpretations of the data that may in fact have heuristic value. In these interpretations we specifically ignore the complex behavior associated with the TI-TII transition seen at 1.6 K (Fig. 4) and focus instead on the evolution of the turbulence from pure superflow to the low line density state TI in thermal counterflow.

One straightforward way to parametrize all of the data is to consider cuts at constant V_n through the dissipation in the V_n-V_s plane. The results obtained from such cuts would appear as the data in Fig. 3. We can approximate these curves by straight lines, where

$$L^{1/2} = \gamma(V_n, T)[V - V_0(V_n, T)] \ . \tag{7}$$

This form for the vortex line density has been used extensively in the literature,[1] although without the explicit V_n dependence of γ and V_0 which is provided by the present experiments. It is possible to fit all of the dissipation data (outside the TI-TII region) to about 10—15% using Eq. (7). The results of these fits are given in Figs. 6 and 7 as

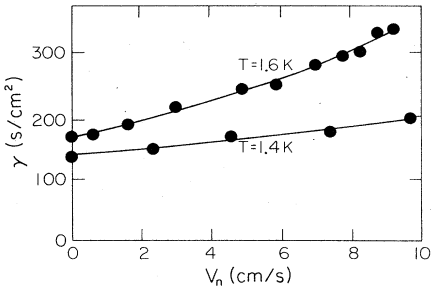

FIG. 6. Values of the coefficient γ in Eq. (7) as a function of V_n for two different temperatures.

the functions γ and V_0. If the results in Figs. 6 and 7 are used in Eq. (7) to generate the vortex line density along the thermal counterflow trajectory we obtain values of $L^{1/2}$ that are slightly nonlinear in V and extrapolate to an intercept somewhat smaller than actually observed. Still, Eq. (7) gives a moderately good representation of the vortex line density in these combined V_n-V_s flows and at least clearly displays the important explicit dependence on the normal-fluid velocity. There are serious conceptual problems associated with an interpretation of the data based upon Eq. (7), however. The vortex line density L is the "equivalent homogeneous line density" obtained from the dissipation using Eqs. (4) and (5). It is difficult to interpret Eq. (5) unless the line density L and the relative velocity V are assumed to be uniform across the flow tube. If the line density is uniform however, the explicit dependence on V_n given by Eq. (7) appears to be without foundation, if not contradictory.

Another interpretation of the data which we find far more attractive is that, in the region of the V_n-V_s plane between superflow and the TI state in thermal counterflow, the vortex line density actually remains at the homogeneous density L_0 found explicitly in superflow, but that Eq. (5) is incomplete. Equation (5) expresses in average macroscopic terms the fact that there is a microscopic dissipative frictional force between a vortex line and normal-fluid excitations. We consider the possibility that in going to the macroscopic average a coupling constant between the lines and the normal-fluid flow is introduced. If we define this coupling constant to be $\alpha(V,V_n)$, then Eq. (5) becomes

$$F_{sn}=\tfrac{2}{3}(\rho_s\rho_n/2\rho)\kappa BVL_0(V)\alpha(V,V_n)\ . \tag{8}$$

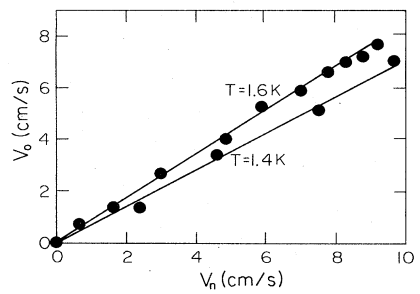

FIG. 7. Values of the intercept V_0 in Eq. (7) as a function of V_n for two different temperatures.

Comparison of Eq. (8) and Eq. (5) indicates that we have absorbed the V_n dependence of the dissipation into the coupling constant α, while the line density is assumed to have the homogeneous value L_0 which only depends on the relative velocity V. In attempting to fit the dissipation data of Figs. 4 and 5, to this modified mutual friction expression, we have considered various cuts through the V_n-V_s plane. The most successful fit of the dissipation was obtained by considering radial cuts in the plane, that is lines of constant V_n/V. The pure superflow and the thermal counterflow trajectories are lines of constant V_n/V. From these cuts we found that the data could be fit well to Eq. (8) by choosing the coupling constant of the form

$$\alpha=(1-aV_n/V)\ , \tag{9}$$

where a is a coefficient that depends on temperature. The degree to which this procedure is successful can be seen in Figs. 8 and 9. Here we have taken the data for the dissipation to calculate F_{sn} from Eq. (4) and used Eq. (8) to calculate the homogeneous line density L_0. The parameter a was varied until the results obtained from different V_n/V cuts converged. For the data at 1.6 K shown in Fig. 8, $a=0.95\pm0.05$. For the data at 1.4 K shown in Fig. 9, $a=0.80\pm0.05$. Clearly the data virtually collapse onto a single line defined by the pure superflow results. The solid line in each figure is Schwarz's result for the line density in a numerical simulation of a homogeneous vortex tangle.[7] Regarded as simply an empirical fit to our dissipation data Eqs. (8) and (9) are quite successful. Combining Eqs. (8) and (9) gives an expression for the mutual friction force that is similar to one proposed by de Haas and van Beelen from a much broader survey of the V_n-V_s plane.[10]

Considering the empirical success of Eqs. (8) and (9) we might take seriously the idea that the line density is actu-

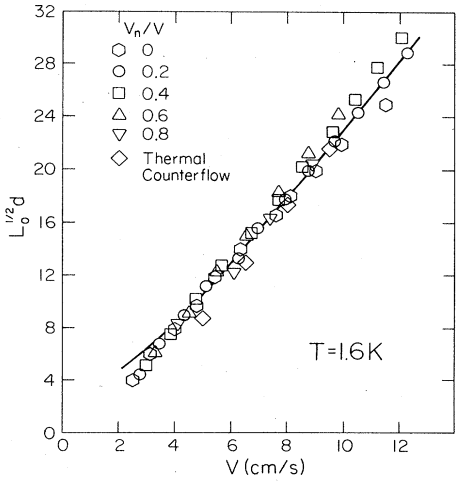

FIG. 8. Homogeneous vortex line density L_0 obtained from the dissipation using Eqs. (8) and (9). Results are shown for a range of V_n/V cuts through the V_n-V_s plane at 1.6 K ranging from pure superflow to thermal counterflow. The solid line is the result of the Schwarz numerical simulation for homogeneous turbulence using $g=0.168$.

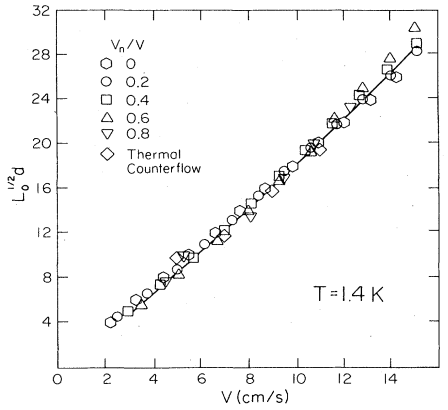

FIG. 9. Homogeneous vortex line density L_0 obtained from the dissipation using Eqs. (8) and (9). Results are shown for a range of V_n/V cuts through the V_n-V_s plane at 1.4 K ranging from pure superflow to thermal counterflow. The solid line is the result of the Schwarz numerical simulation for homogeneous turbulence using $g=0.136$.

ally homogeneous, but that the mutual friction dissipation is reduced by a coupling constant. The factor $\frac{2}{3}$ in Eq. (8) was originally introduced by Vinen[16] to account for the fact that in a homogeneous distribution of vortex lines only about $\frac{2}{3}$ of them would be normal to the direction of the normal fluid velocity and provide dissipation. Perhaps the coupling constant α should be associated with the $\frac{2}{3}$ factor, suggesting a normal-fluid driven polarization of the vortex tangle. When $V_n=0$, $\alpha=1$, and the lines are randomly oriented. For $V_n/V\rightarrow 1$ however, such as for thermal counterflow at low temperatures, $\alpha\rightarrow 0$ implying that the lines would be strongly polarized in the direction of V_n! We consider this to be very unlikely.

Another more appealing interpretation of the coupling constant can be obtained by considering the term αV in Eq. (8) to represent the relative velocity between the normal fluid and the vortex lines (*not* necessarily the superfluid):

$$\alpha V = V_n - V_L \ . \tag{10}$$

Using Eqs. (6) and (9) then gives a vortex line drift velocity of magnitude

$$V_L = V_s - aV_n \ , \tag{11}$$

and suggests that the vortex lines are dragged by the normal fluid. In the absence of the normal fluid drag, $a=0$, $\alpha=1$, and $V_L=V_s$. The assumption that the vortex lines drift with the average superfluid flow V_s is in fact implicit in the unmodified mutual friction expression in Eq. (5).

Our analysis of the dissipation data in the V_n-V_s plane are consistent with a rather simple picture of the superfluid turbulence in combined flows. The vortex line density is maintained at the homogeneous value determined by the relative velocity between the normal fluid and superfluid. The normal-fluid flow produces a drag on the vortex lines which reduces the average velocity between the normal fluid and the lines, reducing the mutual friction dissipation. Ashton and Northby[17] have reported a vortex line drift of this nature although their directly observed drift velocities are about a factor of 3 smaller than would follow from Eq. (11). Awschalom *et al.*[8] have reported a very similar experiment in which no drift of the vortex tangle in the direction of V_n could be detected. In these two experiments, the results were obtained in thermal counterflow well into the *T*II region, and cannot be directly compared to our interpretation of the dissipation data.

Finally we wish to make some remarks about the onset of the *T*II region of superfluid turbulence. This shows up very clearly in the contour plots at 1.6 K in Fig. 4. At 1.4 K our data do not extend to sufficiently large values of V_n to reveal this phenomenon. From the shape of the contours it is clear that the onset of the *T*II region would appear quite abrupt along the thermal counterflow trajectory near $V_n=9$ cm/s, leading to the notion of a critical velocity for the onset of the *T*II state. Several experiments[5,18] have revealed anomalous dynamic behavior of the turbulence near this critical velocity. The contours do not tell us how to extend this critical velocity into the V_n-V_s plane. Indeed, it appears that the phenomenon associated with this transition vanishes continuously as $V_n\rightarrow 0$. The dissipation data taken along the $V_n=5.9$ cm/s trajectory (see Fig. 3), for example, show no evidence of any transition to a higher line density state. It would be interesting to explore the area *above* the thermal counterflow line, where the contours appear to be converging. Data from Leiden indicate that there is locus of points in the first quadrant of the V_n-V_s plane along which the vortex line density changes very abruptly (the "steep branch").[11,12] We are presently modifying our apparatus to allow access to this region. It should also be noted that the *T*I-*T*II transition in thermal counterflow is *not* observed in tubes of high aspect ratio rectangular cross section.[19] Only a single turbulent state with a vortex line density nearly equal to the homogeneous value[8,19] is present in this geometry. The homogeneous state with vortex line density L_0 is present in pure superflow in these same tubes.[3] Consequently, although the dissipation has not been measured in the region of the V_n-V_s plane between superflow and thermal counterflow we can anticipate that the reduced coupling between the normal fluid and the vortex lines will not be present in the rectangular geometry.

ACKNOWLEDGMENT

This work has been supported by the National Science Foundation, Low-Temperature Physics Program, through Grant No. DMR-82-18052.

[1]J. T. Tough, in *Progress in Low Temperature Physics,* edited by D. F. Brewer (North-Holland, Amsterdam, 1982), Vol. 8, p. 133.
[2]R. A. Ashton, L. B. Opatowsky, and J. T. Tough, Phys. Rev. Lett. **46**, 658 (1981).
[3]L. B. Opatowsky and J. T. Tough, Phys. Rev. B **24**, 5420 (1981).
[4]D. R. Ladner, R. K. Childers, and J. T. Tough, Phys. Rev. **B13**, 2918 (1976).
[5]K. P. Martin and J. T. Tough, Phys. Rev. B **27**, 2788 (1983).
[6]J. D. Henberger and J. T. Tough, Phys. Rev. B **23**, 413 (1981).
[7]K. W. Schwarz, Phys. Rev. Lett. **49**, 283 (1982).
[8]D. D. Awschalom, F. P. Milliken, and K. W. Schwarz, Phys. Rev. Lett. **53**, 1372 (1984).
[9]G. van der Heijden, A. G. M. van der Boog, and H. C. Kramers, Physica **77**, 487 (1974).
[10]W. de Haas and H. van Beelen, Physica **83B**, 129 (1976).
[11]R. P. Slegtenhorst and H. van Beelen, Physica **90B**, 245 (1977).
[12]R. P. Slegtenhorst, G. Marees, and H. van Beelen, Physica **113B**, 341 (1982).
[13]R. K. Childers and J. T. Tough, Phys. Rev. B **13**, 1040 (1976).
[14]B. M. Broulik and G. B. Hess, Physica **94B**, 169 (1978).
[15]Marie L. Baehr and J. T. Tough, Phys. Rev. Lett. **53**, 1669 (1984).
[16]W. F. Vinen, Proc. Soc. London, Ser. A **242**, 493 (1957).
[17]R. A. Ashton and J. A. Northby, Phys. Rev. Lett. **30**, 1119 (1973).
[18]C. P. Lorenson, D. L. Griswold, V. U. Nayak, and J. T. Tough, Bull. Am. Phys. Soc. **30**, 534 (1985).
[19]D. R. Ladner and J. T. Tough, Phys. Rev. B **20**, 2690 (1979).